Geodesic Active Regions for Supervised Texture Segmentation*

Nikos Paragios Rachid Deriche
I.N.R.I.A
BP. 93, 2004, Route des Lucioles
06902 Sophia Antipolis Cedex, France
e-mail: {nparagio,der}@sophia.inria.fr

Abstract

This paper presents a novel variational method for supervised texture segmentation. The textured feature space is generated by filtering the given textured images using isotropic and anisotropic filters, and analyzing their responses as multi-component conditional probability density functions. The texture segmentation is obtained by unifying region and boundary-based information as an improved Geodesic Active Contour Model. The defined objective function is minimized using a gradient-descent method where a level set approach is used to implement the obtained PDE. According to this PDE, the curve propagation towards the final solution is guided by boundary and region-based segmentation forces, and is constrained by a regularity force. The level set implementation is performed using a fast front propagation algorithm where topological changes are naturally handled. The performance of our method is demonstrated on a variety of synthetic and real textured frames.

1 Introduction

Texture segmentation, the problem considered in this paper, is one of the most important techniques for image analysis, understanding and interpretation.

The task of texture segmentation is to partition the image into a number of regions such that each region has the same textural properties [7]. Alternatively, this task can be viewed as the problem of accurately extracting the borders between different texture regions in an image [12]. If *a priory* knowledge regarding the textural properties in a given image is available, the problem is called supervised texture segmentation; otherwise it is called un-supervised.

Supervised texture segmentation requires texture analysis and modeling which is usually performed using two well-known techniques; **statistical modeling** [5, 20] and **filtering theory** [2, 11]. Additionally, feature-based image segmentation is performed using either **boundary-based methods** [12, 21] or **region-based methods** [1, 13].

During the last years, there is a significant effort to integrate boundary with region-based segmentation approaches [6, 4, 23]. The difficulty lies on the fact that even though the two modules yield complementary information, they involve conflicting and incommensurate objectives. The region-based methods attempt to capitalize on homogeneity properties, whereas boundary-based ones use the non-homogeneity of the same data as a guide. The most closely related work with this paper can be found in [23], where a two-step variational approach is proposed that combines the geometrical features of a snake/balloon model and the statistical techniques of region growing.

The present work has two main objectives: the first is to propose a complete framework for texture analysis and modeling that combines the filtering theory with the statistical modeling. The second objective is to combine the boundary and the region-based texture segmentation framework into a coupled model, that is derived from the geodesic active contour model. The observation set of this framework is composed of

1. A given set of texture pattern images,
2. A given input frame composed from these patterns.

Following our previous work [18] for supervised texture segmentation using geodesic active contours, we propose a considerable extension that incorporates region-based information to the existing boundary-based information under a coupled framework that can deal with the following problems:

1. The **segmentation of the input frame**, given the background pattern [**fig.** (5.1,5.4)],
2. The extraction of **regions of interest** from the input frame, given the corresponding patterns [**fig.** (5.2,5.3)].

The proposed algorithm is depicted in [**fig.** 1]. Initially, an off-line step is performed that creates multi-component probabilistic texture descriptors for the given set of texture patterns, where the multi-modal data is derived using a set of filter operators [**fig.** 1: *Learning Phase*]. Then, given the input frame, we apply the same operators and derive an observation set that is coherent with the texture descriptors. Then, for each pixel we estimate the probability of being on

*This work was funded in part under the VIRGO research network (EC Contract No ERBFMRX-CT96-0049) of the TMR Program.

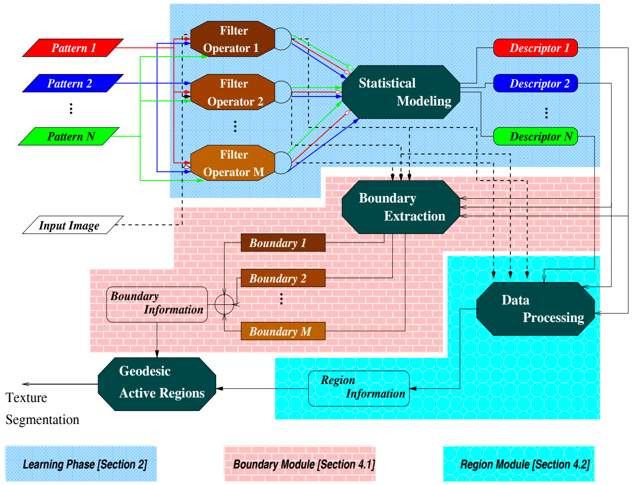

Figure 1. Geodesic Active Regions for supervised texture segmentation

the boundaries between two different texture regions. Since we deal with multi-modal data, a probability vector is obtained. The components of this vector (*e.g.* boundary probabilities) are combined to a single frame using some reliability measurements and provide the **boundary-based** texture information [**fig.** 1: *Boundary Module*]. Besides, using the texture descriptors and the observation set we determine the **region-based** information that is derived from the most probable temporal texture assignment [**fig.** 1: *Region Module*]. Then, the segmentation problem is stated under an improved Geodesic Active Contour model that aims at finding the best minimal length geodesic curve that preserves high boundary probabilities, and creates regions with maximum *a posteriori* segmentation probability with respect to the associated texture hypothesis. We call this model **Geodesic Active Region** model, since boundary and region information are cooperating in a coupled active contour model. The defined objective function is minimized using a gradient-descent method where a level set approach [14] is used to implement the obtained PDE. Finally, the curve propagation problem is implemented using a fast front propagation scheme, the *Hermes Algorithm* [17].

The remainder of this paper is organized as follows. Section 2 deals with the texture analysis and modeling problem while in Section 3, we introduce the main contribution of this paper, the **Geodesic Active Region Model** which is applied to the supervised texture segmentation problem in Section 4. Finally, experimental results and discussion appear in Section 5.

2 Texture Analysis and Modeling

2.1 Extracting Features

In many different applications the use of linear and non-linear filter operators has been applied for feature extraction with quite satisfactory results. Following this example, we adopt a general filter bank composed of:

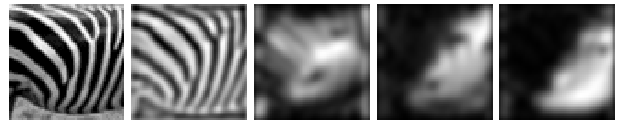

(a) (b) (c) (d) (e)

Figure 2. Filter Operator Responses (a) g(0.5), (b) LoG(0.5), (c) $A\left(1, \frac{\pi}{6}, 0\right)$, (d) $A\left(1, \frac{\pi}{3}, 0\right)$, (e) $A\left(1, \frac{\pi}{3}, \frac{\pi}{6}\right)$.

- The Gaussian operator $\{\mathbf{g}(|\sigma)\}$ [**fig.** (2.a)]

$$\left[g(x, y|\sigma) = \frac{1}{\sqrt{2\pi}\sigma} e^{-\frac{x^2+y^2}{2\sigma^2}} \right]$$

- The isotropic center-surround operator (Laplacian of Gaussian) $\{\mathbf{LoG}(|\sigma)\}$ [**fig.** 2(b)],

$$\left[f(x, y|\sigma) = S\left(1 - \frac{x^2+y^2}{2\sigma^2}\right) e^{-\frac{x^2+y^2}{2\sigma^2}} \right]$$

  where S is a constant scale factor. Besides, the (x, y) anisotropic directional derivatives operators are also considered.

- The 2D Gabor operators analyze the image simultaneously in both space $[\sigma]$, and frequency domains $[\theta, \phi]$.

$$\left[G(x, y|\sigma, \theta, \phi) = \frac{1}{2\pi\sigma^2} e^{-\frac{x^2+y^2}{2\sigma^2}} e^{-j2\pi(\theta x + \phi y)} \right]$$

  These Gabor functions can be decomposed into two components; the real part $[G_R(x, y|\sigma, \theta, \phi)]$ and the imaginary part $[G_I(x, y|\sigma, \theta, \phi)]$. The texture features are captured by the spectrum analyzer $\{\mathbf{A}(|\sigma, \theta, \phi)\}$ of the Gabor components,

$$S(x, y|\sigma, \theta, \phi) = \sqrt{(G_R * I)(x, y)^2 + (G_I * I)(x, y)^2}$$

  smoothed by a Gaussian function [**fig.**(2.[c,d,e])], where $(G_R * I)$ denotes the convolution operation between the image I and the filter G_R.

2.2 Modeling Features

The texture modeling phase aims at finding an appropriate model that can be expressed using a limited set of parameters and preserves strong discrimination power. The most common model related with filtering theory is the use of histograms, where the filter response is discretized using a limited number of values, that affects significantly the extracted model and requires a large set of parameters (histogram cells). We confront these problems, by adopting a statistical framework where the different filter responses (observed histograms) are modeled using continuous probabilities density functions that are Gaussian mixtures [**fig.** 1: *Statistical Modeling*].

In order to facilitate the notation, let us now make some definitions:

- Let $F = \{f_j : j \in [1, \mathtt{M}]\}$ be the set of M preselected filter operators.

- Let $T = \{t_i : i \in [1, \mathtt{N}]\}$ be the set of N texture patterns, and $D = \{\mathbf{D}_i : i \in [1, \mathtt{N}]\}$ be the associated data set.
- And, let $\mathcal{D}(\mathbf{A}) = \{\mathbf{A}_{ij} : i \in [1, \mathtt{N}],\ j \in [1, \mathtt{M}]\}$ be the set of filter operator responses to the input data set, where $\mathbf{A}_{ij}$ is the response of f_j to $\mathbf{D}_i$.

We assume that each filter response can be modeled using low-level statistics, where its observed density function is assumed to be conditional probability. Let $p_{ij}(.)$ be the conditional probability density of the data component $\mathbf{A}_{ij}$. If we assume that this probability density function is homogeneous, *i.e.* independent of the pixel location, then it can be decomposed into many different Gaussian components;

$$p_{ij}(x|\Theta_{ij}) = \sum_{k=1}^{C_{ij}} P_{ij}^k p_{ij}^k(x|\mu_{ij}^k, \sigma_{ij}^k)$$

where C_{ij} is the number of mixture components, P_{ij}^k be the *a priori* probability of the component k, and Θ_{ij} is the vector of the unknown mixture parameters: $\Theta_{ij} = \{(P_{ij}^k, \mu_{ij}^k, \sigma_{ij}^k) : k \in [1, ..., C_{ij}]\}$. The component number is derived automatically form the observed data [18], while the estimation of the unknown parameters is done using the Maximum Likelihood Principle.

The output of this operation is a powerful probabilistic texture description model where each pattern is associated with a vector of probability density functions

- $\mathbf{p}_i(\mathbf{x}) = (p_{i1}(x_1), ..., p_{i\mathtt{M}}(x_{\mathtt{M}}))$

that characterizes its behavior with respect to the different filter operators [**fig.** 1: *Texture Descriptors*].

3 Geodesic Active Regions

The Geodesic Active Contour model has been initially proposed in [3, 8, 10] and successfully applied to a wide variety of computer vision applications. These methods are based on boundary-based information, and aim at finding the best minimal-length smooth curve for a measure derived from the properties of the image.

Besides, motivated by the work proposed in [4, 23], the Geodesic Active Region model has been initially introduced in [16] to deal with the problem of supervised texture segmentation and has been successfully exploited in [19] to deal with the tracking problem. This model is a considerable extension to the geodesic active contour model since it incorporates region-based information and aims at finding a partition where the interior as well as the exterior region preserves the desired image properties.

We are going to introduce this model for a simple segmentation case with two possible decisions. In order to facilitate the notation, let us make some definitions:

- Let $\mathbf{I} : \mathcal{R} \rightarrow \mathbf{R}$ be the input frame.
- Let $\mathcal{P}(\mathcal{R}) = \{\mathcal{R}_A, \mathcal{R}_B\}$ be a partition of the frame domain into two non-overlapping regions $\{\mathcal{R}_A \cap \mathcal{R}_B = \emptyset\}$, where $\mathcal{R}_A$ is the region of interest (hypothesis h_A).
- And, let $\{\partial\mathcal{R}_A\}$ be the $\mathcal{R}_A$ region boundaries.

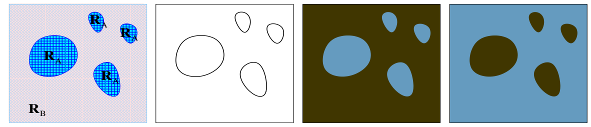

(a) (b) (c) (d)

Figure 3. Geodesic Active Region Model: (a) the input, (b) the boundary-based information,(c,d) the region-based information [proportional to the frame intensity] for hypothesis h_A [c] and for hypothesis h_B [d].

If we assume that for the given frame [**fig.** (3.a)] some information regarding the real region boundaries is available [**fig.** (3.b)], then the extraction of the region of interest can be viewed as the problem of accurately extracting its boundaries.

Let $[\mathbf{p}(\mathbf{I}(\mathbf{s})|\mathbf{B})]$ be the **conditional boundary density function** that measures the probability of a given point being at the real boundaries of $\mathcal{R}_A$. Then, the region of interest can be obtained using the geodesic active contour framework, thus minimizing

$$E(\partial\mathcal{R}_A) = \int_0^1 g(p(\mathbf{I}(\partial\mathcal{R}_A(p)))|B) \left|\partial\dot{\mathcal{R}}_A(p)\right| dp$$

where $\partial\mathcal{R}_A(p) : [0, 1] \rightarrow \mathbf{R}^2$ is a parameterization of the region boundaries in a planar form, and $g()$ is a positive monotonically decreasing function, such that $g(0) = 1$ and $g(x) \rightarrow 0$ as $x \rightarrow \infty$. The solution of the segmentation problem is equivalent with finding the geodesic curve of minimal length that best takes into account the desired image characteristics (important boundary probabilities)[9].

Let us now assume that **an** *a priori* **knowledge about the desired intensity properties of the different regions is available**; the conditional probability density functions $[p_A(\mathbf{I}(s)), p_B(\mathbf{I}(s))]$ with respect to the hypothesis h_A and h_B [**fig.** (3.c,3.d)].

Then, the extraction of the region of interest is equivalent to creating a consistent frame partition between *the observed data, the associated hypothesis and their expected properties*. This partition can be viewed as an optimization problem with respect to the *a posteriori* segmentation probability, given the observation set.

Let $[p(\mathcal{P}(\mathcal{R})|\mathbf{I})]$ be the *a posteriori* segmentation density function with respect to the different partitions $\mathcal{P}(\mathcal{R})$ given the input data $\mathbf{I}$. This density function is given by the Bayes rule as:

$$p(\mathcal{P}(\mathcal{R})|\mathbf{I}) = \frac{p(\mathbf{I}|\mathcal{P}(\mathcal{R}))}{p(\mathbf{I})} p(\mathcal{P}(\mathcal{R}))$$

If we assume that all the partitions are *a priori* equally possible then we can ignore the constant terms $p(\mathbf{I}),\ p(\mathcal{P}(\mathcal{R}))$ and we can rewrite the density function as:

$$p(\mathcal{P}(\mathcal{R})|\mathbf{I}) = p(\mathbf{I}|\{\mathcal{R}_A, \mathcal{R}_B\}) =$$
$$p([\mathbf{I}_A \mid \mathcal{R}_A] \cap [\mathbf{I}_B \mid \mathcal{R}_B]) = p(\mathbf{I}_A \mid \mathcal{R}_A)\ p(\mathbf{I}_B \mid \mathcal{R}_B)$$

Besides, if we assume that the points within each region are independent, we can replace the region probability with:

$$p(\mathbf{I}_X \mid \mathcal{R}_X) = \prod_{s \in \mathcal{R}_X} p_X(\mathbf{I}(s))$$

The maximization of *a posteriori* probability is equivalent with the minimization of the [**-log**()] function of this probability,

$$E(\partial\mathcal{P}(\mathcal{R})) = -\mathbf{log}\left[\prod_{s\in\mathcal{R}_A} p_A(\mathbf{I}(s)) \prod_{s\in\mathcal{R}_B} p_B(\mathbf{I}(s)\right]$$
$$= -\iint_{\mathcal{R}_A} \mathbf{log}\left[p_A(\mathbf{I}(x,y))\right]dxdy - \iint_{\mathcal{R}_B} \mathbf{log}\left[p_B(\mathbf{I}(x,y))\right]dxdy$$

We **fuse the two different segmentation models** by defining the Geodesic Active Region objective function as

$$E(\partial\mathcal{R}_A) = (1-\alpha)\int_0^1 g(p(\mathbf{I}(\partial\mathcal{R}_A(p))))|\partial\dot{\mathcal{R}}_A(p)|dp -$$
$$\alpha\left\{\iint_{\mathcal{R}_A}\mathbf{log}\ [p_A(\mathbf{I}(x,y))]\,dxdy + \iint_{\mathcal{R}_B}\mathbf{log}\,[p_B(\mathbf{I}(x,y))]\,dxdy\right\}$$

The minimization of this function is performed using a gradient descent method. If $u = (x, y)$ is a point of the initial curve (that can belong either to $\mathcal{R}_A$ or to $\mathcal{R}_B$) and we compute the Euler-Lagrange equations [23], then we should deform the curve to this point using the following equation:

$$\frac{du}{dt} = \underbrace{\left[\alpha\mathbf{log}\left(\frac{p_B(\mathbf{I}(u))}{p_A(\mathbf{I}(u))}\right)\right.}_{region\quad term} + \underbrace{\left.(1-\alpha)\left(g(u)\mathcal{K}(u) - \nabla g(u)\cdot\mathcal{N}(u)\right)\right]}_{boundary\quad term}\mathcal{N}(u)$$

where $\mathcal{K}$ is the Euclidean curvature of ∂R_A and $\mathcal{N}$ is the unit inward normal to ∂R_A.

The obtained PDE motion equation has two kind of *forces* acting on the curve, both in the direction of the normal. The **region force** aims at shrink or to expand the curve in the direction that maximizes the *a posteriori* segmentation probability. Thus, if u is a point of h_B $[p_B(\mathbf{I}(u)) > p_A(\mathbf{I}(u))]$ then this force acts to shrink the curve $\left[\alpha\mathbf{log}\left(\frac{p_B(\mathbf{I}(u))}{p_A(\mathbf{I}(u))}\right) > 0\right]$ otherwise acts to expand it. Besides, the **boundary force** contains two sub-terms; one that moves the curve towards the region boundaries constrained by the curvature effect and one that attracts these boundaries (refinement term).

4 Texture Segmentation

We view the segmentation as a frame partition problem [defined by a curve] into non-overlapping regions that preserve *homogeneous textural properties* and *characteristics*. Some complementary definitions are required:

- Let $\mathbf{I}$ be the textured input frame and let $D(\mathbf{I}) = \{\mathbf{I}_j : j \in [1, \mathtt{M}]\}$ be the set of filter responses to this frame.
- Let $\mathcal{P}(R) = \{\mathbf{R}_i : i \in [0, \mathtt{R_N}]\}$ be a partition of frame domain into $\{\mathtt{R_N}+1\}$ non-overlapping regions, where $\mathbf{R}_0$ is the region that corresponds to the *background* pattern.
- Let $\partial\mathcal{P}(R) = \{\partial\mathbf{R}_i : i \in [1, \mathtt{R_N}]\}$ be the region boundaries of the partition $\mathcal{P}(R)$.
- And, let t_{R_i} be the texture pattern that corresponds to the region $\mathbf{R}_i$.

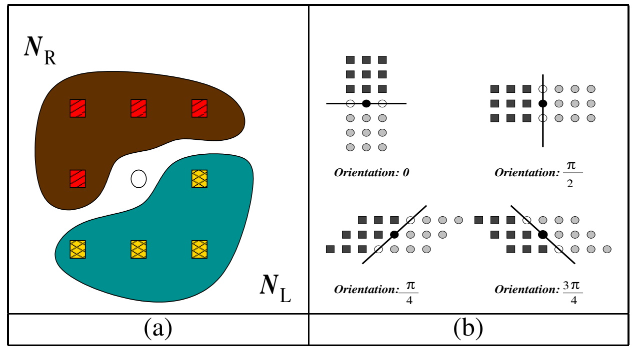

Figure 4. (a) Neighborhood partition that indicates a boundary point, (b) Possible partitions.

4.1 Defining the Boundary Information

It is well known that the extraction of boundary information for textured images is a very tougher task. We propose a probabilistic method to determine this information [18, 22].

Let $N_R(s)$ and $N_L(s)$ be the regions associated with a neighborhood partition, and let $\mathcal{D}(N(s))$ be the corresponding data. Under these assumptions and using the Bayes rule, the probability that s lies on the boundaries between two regions $p(B|\mathcal{D}(N(s)))$ is given by:

$$p(B|D(N(s))) = \frac{p(\mathcal{D}(N(s))|B)}{p(\mathcal{D}(N(s))|B \cup NB)}p(B)$$

where $p(\mathcal{D}(N(s))|B)$ (*resp.* $p(\mathcal{D}(N(s))|NB)$) is the conditional boundary (*resp.* non-boundary) probability and $p(B)$ is the *a priori* boundary probability which is a constant scale factor and can be ignored.

The conditional boundary and (*resp.* non-boundary) probability can be estimated directly from known quantities since *if* s *is a boundary point*, then there is a partition $[N_L(s), N_R(s)]$ where the most probable texture assignment for $N_L(s)$ is the *background* pattern $\{t_{R_0}\}$ and for $N_R(s)$ is a different pattern $\{t_{R_r}\}$ or the opposite. Besides, if s is not a boundary point, then the most probable texture assignment for $N_L(s)$ as well as for $N_R(s)$ is either $\{t_{R_0}\}$ or $\{t_{R_r}\}$. These probabilities are given by [16],

$$\begin{aligned} p(\mathbf{I}(N(s))|B) &= p_{t_{R_0}}(\mathbf{I}(N_R(s)))p_{t_{R_r}}(\mathbf{I}(N_L(s))) \\ &\quad + p_{t_{R_r}}(\mathbf{I}(N_R(s)))p_{t_{R_0}}(\mathbf{I}(N_L(s))) \\ p(\mathbf{I}(N(s))|NB) &= p_{t_{R_0}}(\mathbf{I}(N_R(s)))p_{t_{R_0}}(\mathbf{I}(N_L(s))) \\ &\quad + p_{t_{R_r}}(\mathbf{I}(N_R(s)))p_{t_{R_r}}(\mathbf{I}(N_L(s))) \end{aligned} \quad (1)$$

Since we deal with multi-modal data, each data component can provide boundary-based measurements for a given pixel s. Assuming that the neighborhood partition is known, the boundary probability $p_{j\mathrm{B}}(s|\{\mathbf{I}_j, N, t_{R_r}\})$ for s with respect to the data component $\mathbf{I}_j$ is given by

$$p_{j\mathrm{B}}(s|\{\mathbf{I}_j, N, t_{R_r}\}) = \frac{p_j(\mathbf{I}(N(s))|B)}{p_j(\mathbf{I}(N(s))|B) + p_j(\mathbf{I}(N(s))|NB)}$$

where $p_j(\mathbf{I}(N(s))|B)$ (resp. $p_j(\mathbf{I}(N(s))|NB)$) is derived from [**eq.** (1)]. This probability is defined given a neighborhood partition as well as a texture assignment for the second local region, thus the next problem is to define this partition. We consider four possible neighborhood partitions (the vertical, the horizontal and the two diagonals) [**fig.** (4.b)], obtained by assuming four orientations $\theta = \{0 : \mathbf{0}, \frac{\pi}{4} : \mathbf{1}, \frac{\pi}{2} : \mathbf{2}, \frac{3\pi}{4} : \mathbf{3}\}$; besides, it has been found experimentally that the illustrated in [**fig.** (4.b)] neighborhood size gives very satisfactory results. Finally, to estimate this probability, we need a texture assignment for the second neighborhood region. To overcome this problem, we estimate the boundary probability for all possible partitions and for all possible assignment by generating the matrix

$$P_{\mathtt{B}}(s) = \begin{bmatrix} p_{j\mathtt{B}}(s|\mathbf{0},t_1) & p_{j\mathtt{B}}(s|\mathbf{1},t_1) & p_{j\mathtt{B}}(s|\mathbf{2},t_1) & p_{j\mathtt{B}}(s|\mathbf{3},t_1) \\ \vdots & \vdots & \vdots & \vdots \\ p_{j\mathtt{B}}(s|\mathbf{0},t_k) & p_{j\mathtt{B}}(s|\mathbf{1},t_k) & p_{j\mathtt{B}}(s|\mathbf{2},t_k) & p_{j\mathtt{B}}(s|\mathbf{3},t_k) \\ \vdots & \vdots & \vdots & \vdots \\ p_{j\mathtt{B}}(s|\mathbf{0},t_{\mathtt{N}}) & p_{j\mathtt{B}}(s|\mathbf{1},t_{\mathtt{N}}) & p_{j\mathtt{B}}(s|\mathbf{2},t_{\mathtt{N}}) & p_{j\mathtt{B}}(s|\mathbf{3},t_{\mathtt{N}}) \end{bmatrix}$$

where the lines correspond to the possible texture assignments $\{t_1, ..., t_{t_{R_0}-1}, t_{t_{R_0}+1}, ..., t_{\mathtt{N}}\}$ and the columns to the different neighborhood partitions $\{\mathbf{0}, \mathbf{1}, \mathbf{2}, \mathbf{3}\}$. The element (m, n) of this matrix, corresponds to the boundary probability of partition n if the second local region is assigned to the texture hypothesis t_m.

This operation provides $\{\mathtt{M}\}$ boundary probability frames (one for each data component $\{\mathbf{I}_j\}$) that have to be combined to a single frame. This can be done using the mean value between the different frames, but it is not the most proper solution since the quality of the boundary maps differs from data component to data component. We introduce a reliability measurement for each boundary map, which is associated with the discrimination power of the corresponding filter with respect to the *background* pattern.

At the end of the analysis and modeling phase, we have associated to each pattern, a descriptor, which given a value and its nature (data component) returns the probability of being part of this descriptor. A filter operator has strong discrimination power, if all the observed values of the corresponding *background* data component are being correctly classified, (*e.g.* the probability with respect to the *background* pattern is superior to the probability with respect to any other pattern). The probability of being correct $P_j(C)$ with respect to the filter f_j is equivalent to an observation x being classified as the *background* texture pattern t_{R_0}, where the true state of nature is t_{R_0}. As a consequence, for each filter operator f_j we have

$$P_j(C) = P\left(x \in \mathbf{D}_{t_{R_0}j} \cap \left[p_{t_{R_0}j}(x) \geq p_{ij}(x) : \forall j \in [0, \mathtt{M}]\right]\right) \iint_{\mathbf{D}_{t_{R_0}j}} p_{t_{R_0}j}(\mathbf{D}_{t_{R_0}j}(x,y)) H\left(\mathbf{D}_{t_{R_0}j}(x,y)\right) dxdy$$

where $H(x, j) : R \times [0, \mathtt{N}], \to R$ is a binary function given by,

$$H(a, j) = \begin{cases} 1 & , \quad \textit{if} \ \ p_{t_{R_0}j}(a) \geq p_{ij}(a); \forall i \in [0, \mathtt{N}] \\ 0 & , \quad \textit{otherwise} \end{cases}$$

We normalize the reliability measurements $[P_j(C)]$ with respect to the different filter operators $\left[\mathbf{w}_j = \frac{P_j(C)}{\sum_{k=1}^{\mathtt{M}} P_k(C)}\right]$ and we use them to generate a global boundary matrix that combines the different filter responses:

$$P_{\mathtt{B}}(s) = \begin{bmatrix} \sum_j^{\mathtt{M}} w_j \ p_j(s|\mathbf{0}, t_1) & \sum_j^{\mathtt{M}} w_j \ p_i(s|\mathbf{3}, t_1) \\ & \vdots & \\ \sum_j^{\mathtt{M}} w_j \ p_j(s|\mathbf{0}, t_{\mathtt{N}}) & \sum_j^{\mathtt{M}} w_j \ p_j(s|\mathbf{3}, t_{\mathtt{N}}) \end{bmatrix}$$

The **boundary probability** $p_{\mathbf{B}}(s)$ for the pixel s is then provided by the highest element of the matrix $P_{\mathtt{B}}(s)$.

4.2 Defining the Region Information

Let $p(\mathcal{P}(R)|D(R))$ be the *a posteriori* segmentation probability with respect to the partition $\mathcal{P}(R)$. Since the *a posterior* region probabilities $p\left(D(\mathbf{R}_i)|t_{R_i}\right)$ are independent, the global *a posteriori* segmentation probability is given by,

$$p(\mathcal{P}(R)|D(\mathbf{I})) = p\left(\cap_{i=0}^{\mathtt{R_N}} \left[D(\mathbf{R}_i)|t_{R_i}\right]\right) = \prod_{i=0}^{\mathtt{R_N}} p\left(D(\mathbf{R}_i)|t_{R_i}\right)$$

where $D(\mathbf{R}_i)$ is the multi-modal data associated with the region R_i. The use of multi-modal data drives to multi-variate conditional probabilities. If we assume independence between the different filter responses, then the *a posteriori* segmentation probability is given by

$$p(\mathcal{P}(R)|D(\mathbf{I})) = \prod_{i=0}^{\mathtt{R_N}} \prod_{j=1}^{\mathtt{M}} p\left(\mathbf{I}_j(\mathbf{R}_i)|t_{R_i}\right)$$

where $p\left(\mathbf{I}_j(\mathbf{R}_i)|t_{R_i}\right)$ is the *a posterior* segmentation probability for the region $\{\mathbf{R}_i\}$ with the respect to the data component $\{\mathbf{I}_j\}$.

4.3 Setting the Energy

Although we made the assumption that the different filter responses are independent, they have some uncertainty measurements, since we use a global statistical model to describe their behavior. These uncertainties are expressed from the discrimination power of the corresponding filters $\{w_j\}$.

The geodesic active region functional for supervised texture segmentation consists of minimizing

$$E(\partial\mathcal{P}(R)) = (1-\alpha) \sum_{i=1}^{\mathtt{R_N}} \int_0^1 g(p_{\mathbf{B}}(\partial\mathbf{R}_i(p_i))) |\partial\dot{\mathbf{R}}_i(p_i)| dp - \alpha \sum_{i=0}^{\mathtt{R_N}} \iint_{\mathcal{R}_i} \sum_{j=1}^{\mathtt{M}} w_j \ \mathbf{log}\left[p_{t_{R_i}j}(\mathbf{I}_j(x,y))\right] dxdy$$

where $g()$ is a Gaussian function.

4.4 Minimizing the Energy

Let $u = (x, y)$ be a point of the initial curve. This point can either be at region R_0 or at region R_k. Based on this hypothesis, we compute the Euler-Lagrange equations [3, 23] (Section 2), and we derive the following motion equation for u:

$$\frac{du}{dt} = \left[\alpha \sum_{j=1}^{M} w_j \, \mathbf{log}\left(\frac{p_{t_{R_0}j}(\mathbf{I}_j(u))}{p_{t_{R_k}j}(\mathbf{I}_j(u))}\right) + (1-\alpha)\left(g(p_{\mathbf{B}}(u))\mathcal{K}(u) - \nabla g(p_{\mathbf{B}}(u)) \cdot \mathcal{N}(u)\right)\right]\mathcal{N}(u)$$

The interpretation of the above PDE is obvious. Given a initial curve, it creates a partition of the image [determined by a curve that attracts the region boundaries] where the exterior curve region corresponds to the *background* pattern while the interior regions correspond to the other patterns.

The obtained PDE can be implemented using a Lagrangian approach, that is limited since it cannot deal with topological changes of the moving front and suffers from instability in the domain of numerical approximations.

This can be avoided by introducing the work of Osher and Sethian [14] in our scheme. The central idea is to represent the moving front $\partial R(t)$ as the zero-level set $\{\Phi = 0\}$ of a function Φ. This representation of $\partial R(t)$ is implicit, parameter-free and intrinsic. Additionally, it is topology-free.It is easy to show, that if the embedding function Φ deforms according to

$$\frac{d}{dt}\Phi(p,t) = \mathcal{F}(p)\,|\nabla\Phi(p,t)|$$

then the corresponding moving front evolves according to:

$$\frac{d}{dt}C(p,t) = \mathcal{F}(p)\mathcal{N}$$

Thus, the minimization of the proposed geodesic active region objective function is equivalent to searching for a steady-state solution of the following equation:

$$\frac{d}{dt}\Phi(u) = \left[\alpha \sum_{j=1}^{M} w_j \, \mathbf{log}\left(\frac{p_{t_{R_0}j}(\mathbf{I}_j(u))}{p_{t_{R_k}j}(\mathbf{I}_j(u))}\right) + (1-\alpha) \left(g(p_{\mathbf{B}}(u))\mathcal{K}(u) + \nabla g(p_{\mathbf{B}}(u)) \cdot \frac{\nabla\Phi(u)}{|\nabla\Phi(u)|}\right)\right]|\nabla\Phi(u)|$$

where the geometric properties are estimated directly from the level set frame.

The Level Set Equation is implemented using the **Hermes** algorithm [17, 15] that proposes a fast way to deform the initial curve locally towards the minimum of the objective function.

4.5 Implementation Issues

The proposed method can be used to segment a given texture frame, in the case where the *background* texture pattern is known [**fig.** (5.1,5.4)]. This method can be easily extend to extract some specific regions of interest determined by the corresponding *preferable* patterns [**fig.** (5.2,5.3)]. In both cases, the curve propagation requires a texture assignment for the given point that has to be compared with the *preferable* assignments. This issue is confronted by assuming that the temporal segmentation map is derived by the most probable texture assignments. Thus for a given curve point, we assume that it is located between the *preferable* region and the region that corresponds to the most probable assignment (which is derived from the observed data).

5 Conclusions, Results

Synthetic data [**fig.** (5.1)], as well as real-word data [**fig.** (5.2, 5.3, 5.4)] have been used to test and validate the proposed approach [1].

Summarizing, we have considered a curve propagation approach for supervised texture segmentation. The main contribution of our approach is the proposition of **a coupled variational energy framework which integrates boundary-based and region-based information modules and connects the minimization of the objective function with the curve propagation theory**, namely the **Geodesic Active Region** framework. This framework was successfully applied to the supervised texture segmentation problem, where the boundary information is determined using a probabilistic framework, while the region-based information is expressed directly via conditional probabilities. The quality of this information is ensured by the use of powerful probabilistic texture descriptors (learning phase) that combine filtering theory and statistical modeling. The proposed model preserves robustness, and is *independent* from the initialization step thanks to the level set implementation and to the region-based term which creates data-dependent positive and negative propagation forces.

The proposed model is not limited to texture segmentation, but it can be used to deal with a wide variety of computer vision applications that can be reformulated as frame partition problems. The future direction of this work is to validate the proposed model to other computer vision domains.

An extended version of this paper can be found in [16]. Various experimental results (in MPEG format), including the ones shown in this article, can be found at:
http://www.inria.fr/robotvis/personnel/nparagio/demos/
http://www.inria.fr/robotvis/personnel/der/der-eng.html

---

[1] The segmentation performance of our method is demonstrated in [**fig.** (5.1, 5.4)]. Additionally, the performance with respect to the extraction of region of interest is demonstrated in [**fig.** (5.2, 5.3)] where the patterns of interest are given (zebra, chita). Each demonstration contains information about the modeling phase (patterns and filter operators). The filter operators are selected manually, and their size is either 7x7, or 9x9, or 11x11.

The independence of our method with respect to the initialization step is clearly demonstrated. As it concerns the curve propagation, in the case of the absence of curvature, it follows the normal direction (the boundary force is not valid, and the region force is not affected by the curvature), while the presence of curvature aims at creating a smooth curve propagation sequence.

Finally, the computational cost of our approach is related with the initialization step, and varies between 2 and 5 seconds using an ULTRA 10, 299 MHz (the learning phase is not included).

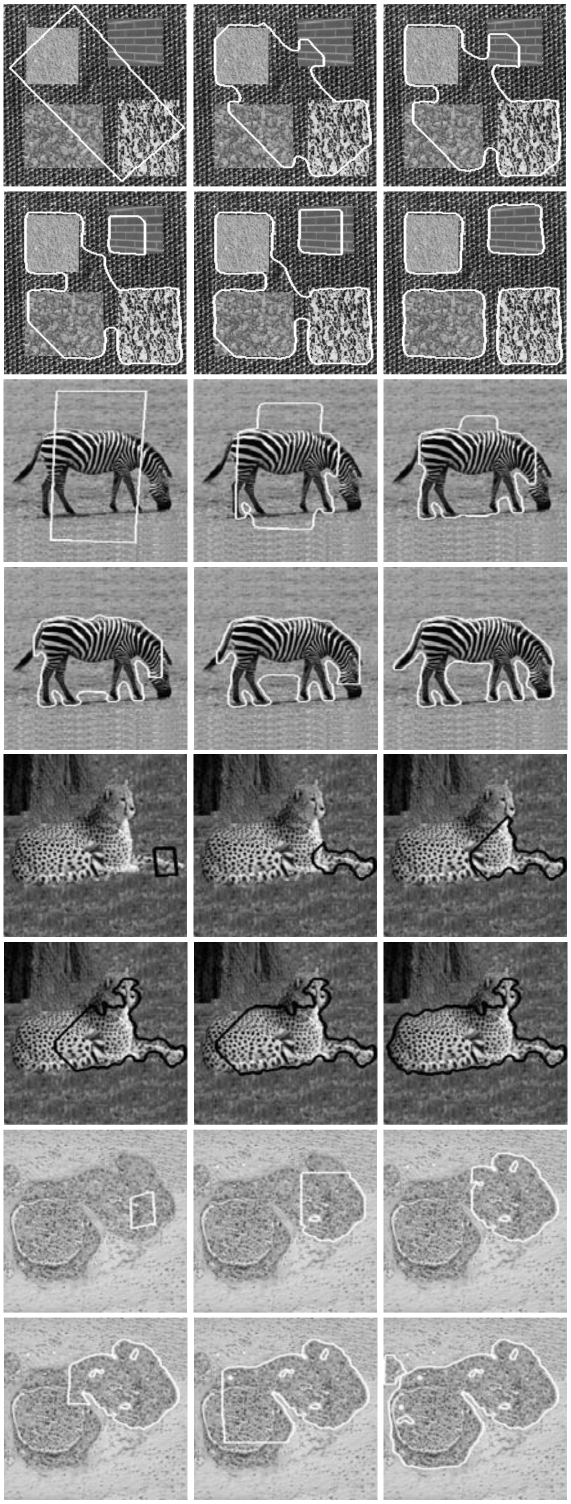

Figure 5. (1) Patterns: *5*, filters: *5* S(1), LoG(1), A$[(1, 2\pi, 2\pi)$, A$(1, \frac{\pi}{6}, 0)$, A$(1, \frac{\pi}{2}, \frac{\pi}{3})$. (2) Patterns: *3*, filters: *6* S(1), derivatives, A$[(1, 2\pi, 2\pi)$, A$(1, \frac{\pi}{6}, 0)$, A$(1, \frac{\pi}{3}, 0)$, A$(1, 0, \frac{\pi}{3})]$. (3) Patterns: *3*, filters: *8* S(1), GsA$[(1, 2\pi, 2\pi, 0)$, A$(1, \frac{\pi}{6}, 0)$, A$(1, \frac{\pi}{3}, 0)$, A$(1, 0, \frac{\pi}{3})$, A$(1, 0, \frac{\pi}{6})$, A$(1, \frac{\pi}{6}, \frac{\pi}{3})$, A$(1, \frac{\pi}{3}, \frac{\pi}{6})]$. (4) Patterns: *3*, filters: *9* S(1), LoG(1), A$[(1, 2\pi, 2\pi, 0)$, A$(1, \frac{\pi}{6}, 0)$, A$(1, \frac{\pi}{3}, 0)$, A$(1, 0, \frac{\pi}{3})$, A$(1, 0, \frac{\pi}{6})$, A$(1, \frac{\pi}{3}, \frac{\pi}{3})$, A$(1, \frac{\pi}{6}, \frac{\pi}{6})]$.

References

[1] R. Adams and L. Bischof. Seeded Region Growing. *IEEE PAMI*, 16:641–647, 1994.

[2] A. Bovik, M. Clark, and W. Geister. Multichannel texture analysis using localized spatial filters. *IEEE PAMI*, 12:55–73, 1990.

[3] V. Caselles, R. Kimmel, and G. Sapiro. Geodesic active contours. *IJCV*, 22:61–79, 1997.

[4] A. Chakraborty, H. Staib, and J. Duncan. Deformable Boundary Finding in Medical Images by Integrating Gradient and Region Information. *IEEE Transactions on Medical Imaging*, 15(6):859–870, 1996.

[5] P. Chen and T. Pavlidis. Segmentation by texture using correlation. *IEEE PAMI*, 5:64–69, 1983.

[6] J. Haddon and J. Boyce. Inage Segmentation by Unifying Region and Boundary Information. *IEEE PAMI*, 12:929–948, 1990.

[7] A. Jain and F. Farrokhnia. Unsupervised texture segmentation using Gabor filters. *Pattern Recognition*, 24:1167–1186, 1991.

[8] S. Kichenassamy, A. Kumar, P. Olver, A. Tannenbaum, and A. Yezzi. Gradient flows and geometric active contour models. In *IEEE ICCV*, pages 810–815, Boston, USA, 1995.

[9] S. Kichenassamy, A. Kumar, P. Olver, A. Tannenbaum, and A. Yezzi. Conformal curvature flows: from phase transitions to active vision. *Archive of Rational Mechanics and Analysis*, 134:275–301, 1996.

[10] R. Malladi, J. Sethian, and B. Vemuri. Shape modeling with front propagation: A level set approach. *IEEE PAMI*, 17:158–175, 1995.

[11] S. Mallat. Multiresolution approximations and wavelet orthonormal bases of $L^2(R)$. *Trans. Amer. Math. Soc.*, 315:69–87, 1989.

[12] B. Manjunath and R. Chellapa. A Computational Approach to boundary detection. In *IEEE CVPR*, pages 358–362, 1991.

[13] B. Manjunath and R. Chellapa. Unsupervised texture segmentation using Markov Random Field models. *IEEE PAMI*, 13:478–482, 1991.

[14] S. Osher and J. Sethian. Fronts propagating with curvature-dependent speed : algorithms based on the hamilton-jacobi formulation. *Journal of Computational Physics*, 79:12–49, 1988.

[15] N. Paragios. *Geodesic Active Regions and Level Sets: Contributions and Applications in Artificial Vision*. PhD thesis, University of Nice/Sophia Antipolis, France, November 1999. http://www-sop.inria.fr/robotvis/personnel/nparagio/thesis.

[16] N. Paragios and R. Deriche. Geodesic Active Regions for Texture Segmentation. Research Report 3440, INRIA, France, 1998. http://www.inria.fr/rapports/sophia/RR-3440.html.

[17] N. Paragios and R. Deriche. A PDE-based Level Set approach for Detection and Tracking of moving objects. In *IEEE ICCV*, pages 1139–1145, Bombay, India, 1998.

[18] N. Paragios and R. Deriche. Geodesic Active Contours for Supervised Texture Segmentation. In *IEEE CVPR*, Colorado, USA, 1999.

[19] N. Paragios and R. Deriche. Unifying Boundary and Region-based Information for Geodesic Active Tracking. In *IEEE CVPR*, Colorado, USA, 1999.

[20] M. Unser. Local linear transforms for texture measurements. *Signal Processing*, 11:61–79, 1986.

[21] S. Yhann and T. Young. Boundary localization in texture segmentation. *IEEE IP*, 4:849–856, 1995.

[22] X. Zeng, L. Staib, R. Schukz, and J. Duncan. Volumetric Layer Segmentation Using Coupled Surfaces Propagation. In *IEEE CVPR*, pages 708–715, Santa Barbara, USA, 1998.

[23] S. Zhu and A. Yuille. Region Competition: Unifying Snakes, Region Growing, and Bayes/MDL for Multiband Image Segmentation. *IEEE PAMI*, 18:884–900, 1996.